

Optimal representations of quantum states by Gaussians in phase space

Anatole Kenfack^{1,2}, Jan M Rost¹ and Alfredo M Ozorio de Almeida³

¹ Max Planck Institute for the Physics of Complex Systems, Nöthnitzer Strasse 38, 01187 Dresden, Germany

² The University of Dschang, Faculty of Science, Physics Department, PO Box 67, Dschang, Cameroon

³ Centro Brasileiro de Pesquisas Físicas, R Xavier Sigaud 150, 22290-180 Rio de Janeiro, Brazil

E-mail: kenfack@mpipks-dresden.mpg.de

Received 14 November 2003

Published 7 April 2004

Online at stacks.iop.org/JPhysB/37/1645 (DOI: 10.1088/0953-4075/37/8/007)

Abstract

A two-step optimization is proposed to represent an arbitrary quantum state to the desired accuracy with the smallest number of Gaussians in phase space. The Husimi distribution of the quantum state provides the information to determine the modulus of the weight for the Gaussians. Then, the phase information contained in the Wigner distribution is used to obtain the full complex weights by considering the relative phases for pairs of Gaussians, the chords. The method is exemplified with excited states n of the harmonic and the Morse oscillators. A semiclassical interpretation of the number of Gaussians needed as a function of the quantum number n is given.

(Some figures in this article are in colour only in the electronic version)

1. Introduction

Wigner representation of quantum states has been of interest in various fields of physics with correspondingly different motivations. In physical chemistry, e.g., one aims at formulating a quantum initial state in terms of a Wigner distribution constructed with Gaussians since their centres serve as initial conditions for a classical propagation of the system of interest in time. In quantum optics, e.g., a state of the electromagnetic (EM) field has been formulated as a Wigner distribution constructed with Gaussians. Here, one is interested in creating special states of the EM field by mixing coherent states appropriately which can be experimentally produced. Consequently, the approaches have been very different in the two cases: in the first example, Monte Carlo sampling of initial centres for Gaussians has been used with a subsequent fitting of the coefficients of the Gaussians [1]. Making use of time reversal symmetry, only real coefficients were necessary. In the second example, the Gaussian basis has also been restricted to a one-dimensional manifold, either by putting the Gaussians on

a line or on a circle [2]. In this case, however, the (complex) coefficients can be directly determined using the analytical properties of coherent states.

Here, we aim at combining the flexibility of using arbitrarily placed Gaussians available in the first example with the rigour of determining the coefficients of the Gaussian basis functions in a one-dimensional manifold of the second example. To this end, we first formulate in section 2 a Wigner phase space representation of a quantum state in terms of an expansion into Gaussians. Smoothing the distribution leads to the Husimi representation and allows us to determine the squared moduli A_j of the coefficients for the Gaussians by diagonalization, since the (off-diagonal) oscillatory part is highly suppressed by the smoothing, as explained in section 2. Yet, as can be shown, the A_j are the same as in the Wigner representation. Hence, we can insert the A_j into the Wigner representation and determine from its Fourier transform in phase space the phases θ_j to finally get the full complex coefficients

$$a_j = (A_j 2\pi\hbar)^{1/2} \exp i\theta_j, \quad (1)$$

up to a global (arbitrary) phase. At this point, we come back to a one-dimensional manifold in phase space, as in example 2 above. However, we cannot use a predefined path (such as a line or circle). Instead, we make use of the chord representation which consists of all pairs of the Gaussians, as detailed in section 3. A polygon of a subset of chords, which are independent of each other and have the largest distances in phase space, is the most reliable and sufficient to obtain the phases. The polygon forms a one-dimensional manifold in phase space as in example 2, and allows for fully flexible (i.e. randomly placed Gaussians) as in example 1. Additionally, the coherent state basis determined in this way carries optimized, complex weights.

In section 4, we demonstrate how the proposed construction actually performs, using excited harmonic and Morse oscillator states as examples. In section 5, we provide a semiclassical interpretation of the number of Gaussians needed in terms of the degree of excitation (number of nodes) to represent the states to a given accuracy. The paper ends with a conclusion in section 6.

2. Wigner and Husimi representations in terms of Gaussians

We start from the Wigner representation

$$W^\psi(x) = \int \frac{dq'}{2\pi\hbar} \left\langle q + \frac{q'}{2} \middle| \psi \right\rangle \left\langle \psi \middle| q - \frac{q'}{2} \right\rangle \exp\left(-\frac{i}{\hbar} p q'\right), \quad (2)$$

of a quantum state ψ where $x = (p, q)$ is an abbreviation for momentum p and position q .

We may expand the quantum state in a coherent state basis of finite length N ,

$$|\psi\rangle \approx \sum_{j=1}^N a_j |X_j\rangle, \quad (3)$$

where the $|X_j\rangle$ are coherent states centred at (P_j, Q_j) which read in position representation [3, 4]

$$\langle q | X_j \rangle = (\pi\hbar)^{-1/4} \exp\left(-\frac{1}{2\hbar}(q - Q_j)^2 + \frac{i}{\hbar} P_j(q - Q_j/2)\right). \quad (4)$$

Increasing N , the quantum state can be represented with high accuracy by (3), only limited by numerical instabilities once the momenta become too large. Inserting (3) into the Wigner representation (2), one obtains

$$W^\psi(x) = \sum_{j,k=1}^N a_j a_k^* W_{jk}(x), \quad (5)$$

where

$$W_{jk}(x) \equiv W(X_j, X_k, x) = \int \frac{dq'}{2\pi\hbar} \left\langle q + \frac{q'}{2} \left| X_j \right. \right\rangle \left\langle X_k \left| q - \frac{q'}{2} \right. \right\rangle \exp\left(-\frac{i}{\hbar} p q'\right). \quad (6)$$

With (4) the integration over q' in (6) can be performed to arrive at the explicit expression

$$W_{jk}(x) = \frac{1}{\pi\hbar} \exp(-(x - \bar{X}_{jk})^2/\hbar) \exp\left(-\frac{i}{\hbar}(x \wedge \delta X_{jk} + X_j \wedge X_k/2)\right), \quad (7)$$

known as the crossed Wigner function (or Moyal bracket [5]), where

$$\bar{X}_{jk} = (X_j + X_k)/2 \quad \text{and} \quad \delta X_{jk} = X_j - X_k. \quad (8)$$

In (7) we have used the wedge product,

$$X \wedge X' = P Q' - Q P' \equiv (\mathbf{J}X) \cdot X', \quad (9)$$

to shorten the notation. (With the equivalence in (9) we also define the symplectic matrix \mathbf{J} .)

The oscillating W_{jk} for $j \neq k$ have a contribution from a Gaussian centred half way between X_j and X_k at \bar{X}_{jk} , which is as strong as the (non-oscillating) diagonal contributions W_{jj} centred at X_j . Although the Wigner representation W^ψ in terms of N Gaussians becomes exact for $N \rightarrow \infty$, it is numerically tedious to determine the complex a_j , even for a finite number N of terms in (5), due to the strong oscillations in W^ψ . Hence, we smooth W^ψ in the well-known fashion to arrive at the Husimi representation

$$\begin{aligned} H^\psi(x) &= (\pi\hbar)^{-1} \int dx' \exp(-(x - x')^2/\hbar) W^\psi(x') \\ &= \frac{1}{2\pi\hbar} \sum_{j,k} a_j a_k^* \langle x|X_j\rangle \langle X_k|x\rangle, \end{aligned} \quad (10)$$

where

$$\langle x|X_k\rangle = \exp\left(-\frac{1}{4\hbar}(x - X_k)^2 - \frac{i}{2\hbar}x \wedge X_k\right). \quad (11)$$

Now, the oscillations in the off-diagonal terms have a wavelength of $2\pi\hbar/|\delta X_{jk}|$ in phase space. Hence, they are damped exponentially with increasing separation δX_{jk} of the Gaussians. This justifies the use of only the diagonal part of H^ψ to determine the coefficients $A_j = |a_j|^2/(2\pi\hbar)$ in

$$H^\psi(x) \approx \bar{H}^\psi(x) = \sum_{j=1}^N A_j |\langle x|X_j\rangle|^2, \quad (12)$$

where we call

$$|\langle x|X_j\rangle|^2 = \exp\left(-\frac{1}{2\hbar}(x - X_j)^2\right), \quad (13)$$

a Gaussian phase space packet (gpp).

3. Optimization of the Gaussian (gpp) representation

3.1. Obtaining the moduli by matrix diagonalization from the Husimi function

Assuming that the locations $x_{j=1,\dots,N}$ are given (the Monte Carlo procedure will be illustrated in section 4 with an example) we minimize the functional

$$\sigma[A_{[j]}, N] = \int dx \left(H^\psi(x) - \sum_{j=1}^N A_j |\langle x|X_j\rangle|^2 \right)^2, \quad (14)$$

in the $A_{\{j\}}$. The minimization turns into a linear optimization problem by discretizing the integral on a grid with L phase space points $x_{l=1,\dots,L}$,

$$\sigma_L[A_{\{j\}}, N] = \frac{1}{N_L} \sum_{l=1}^L \left(H^\psi(x_l) - \sum_{j=1}^N A_j |\langle x_l | X_j \rangle|^2 \right)^2 \equiv \sum_{l=1}^L s(x_l), \quad (15)$$

with the normalization $N_L = \sum_{l=1}^L (H^\psi(x_l))^2$. As can be easily seen, $\sigma_L[A_{\{j\}}, N]$ is minimized by solving the matrix equation

$$\mathbf{G}\mathbf{A} = h^\psi, \quad (16)$$

where the matrix elements $G_{lj} = |\langle x_l | X_j \rangle|^2$ are gpps. The vector $\mathbf{A} = (A_1, A_2, \dots, A_N)$ contains the coefficients to be determined and the vector h^ψ is the discretized Husimi function with elements $h_j^\psi = H^\psi(x_j)$. In general, the matrix G will be sparse and appropriate algorithms can be used to solve (16) efficiently [6].

3.2. Obtaining the phases from the largest chords in the chord function

Having determined the A_j we still lack the phases θ_j of the coefficients in (1). While the smoothed distribution H^ψ suppresses the interference terms caused by the phases, we now need a representation which does the exact opposite: emphasizing the phase differences over the diagonal contributions. In general, this is not possible since the diagonal contributions dominate in the Wigner representation (5). However, we can separate the location of the diagonal contributions from that of the off-diagonal terms in phase space. This is accomplished by taking the *phase space Fourier transform* of the Wigner representation $W^\psi(x)$ defined by

$$\tilde{W}^\psi(\xi) = \int \frac{dx}{2\pi\hbar} W^\psi(x) \exp\left(\frac{i}{\hbar}(x \wedge \xi)\right), \quad (17)$$

which is also called the chord function [7].⁴ The chord function \tilde{W}^ψ is given in the coherent state basis by

$$\tilde{W}^\psi(\xi) = \sum_{j,k=1}^N a_j a_k^* \tilde{W}_{jk}(\xi), \quad (18)$$

where

$$\tilde{W}_{jk}(\xi) \equiv \tilde{W}(X_j, X_k, \xi) = \int \frac{dq}{2\pi\hbar} \left\langle q + \frac{\xi_q}{2} \middle| X_j \right\rangle \left\langle X_k \middle| q - \frac{\xi_q}{2} \right\rangle \exp\left(-\frac{i}{\hbar} \xi_p q\right), \quad (19)$$

with $\xi = (\xi_p, \xi_q)$. In the representation (18) it is easy to see that the chord function is related to the original $W_{jk}(x)$ from (6) through

$$\tilde{W}(X_j, X_k, \xi) = \frac{1}{2} W(X_j, -X_k, \xi/2), \quad (20)$$

which can be used in connection with (7) to obtain directly

$$\tilde{W}_{jk}(\xi) = \frac{1}{2\pi\hbar} \exp\left(-\frac{(\xi - \delta X_{jk})^2}{4\hbar}\right) \exp\left(-\frac{i}{\hbar}(\xi \wedge \bar{X}_{jk} + X_k \wedge X_j/2)\right). \quad (21)$$

Hence, the phase space Fourier transform turns X_k into $-X_k$ in the coherent state representation which means that sums \bar{X}_{kj} and differences δX_{jk} of Gaussians interchange their role, going from W_{jk} to \tilde{W}_{jk} . As one can see from (21) all diagonal terms $j = k$ collapse onto Gaussians

⁴ Usually the sign of ξ_p is reversed in the definition of \tilde{W}^ψ , known as the Woodward ambiguity function in communication theory [8] or the characteristic function in quantum optics [9]. Here we follow the definition from [7].

centred at $\xi = 0$, whereas each interference term is a Gaussian centred on the *chord* δX_{jk} joining X_j and X_k . (Both directions $\pm\delta X_{jk}$ are present, leading to symmetric contributions in chord space with $\tilde{W}(-\xi) = \tilde{W}^*(\xi)$.) The complementary purpose of the chords compared to the original Gaussians, emphasizing diagonal and off-diagonal properties of the Wigner representation, respectively, has its reason in the replacement of all midpoint centres \bar{X}_{jk} by differences δX_{jk} and vice versa in the Gaussians.

To finally obtain the phases we look for a chord δX_{jk} which is sufficiently far from all the other chords, so that at $\xi = \delta X_{jk}$ the chord function is dominated by the single nondiagonal contribution $\tilde{W}_{jk}(\delta X_{jk})$:

$$\begin{aligned} \tilde{W}^\psi(\delta X_{jk}) - \sum_l |a_l|^2 \tilde{W}_{ll}(\delta X_{jk}) &\approx a_j a_k^* \tilde{W}_{jk}(\delta X_{jk}) \\ &= \sqrt{A_j A_k} \exp(i(\theta_{jk} - X_k \wedge X_j / 2\hbar)). \end{aligned} \quad (22)$$

Recalling that we have already determined A_j from the Husimi function, we can solve (22) for $\theta_{jk} = \theta_j - \theta_k$. Of course, the modulus of both sides of (22) should be approximately equal, which provides a check on the previous Husimi fitting. The diagonal sum that is subtracted from $\tilde{W}^\psi(\delta X_{jk})$ in (22) decays exponentially with δX_{jk}^2 , so it will only affect the phases of the smaller chords. It might appear to only be consistent with our previous approximation of the Husimi function to neglect the diagonal sum in (22), but this would perturb the phases of small chords.

4. Placing the Gaussians: examples

So far, nothing has been said about how to place the Gaussians in phase space that are meant to approximate a given Husimi function. An obvious criterion is that any relative maximum of this smooth distribution should also receive a coherent state. Further knowledge of the distribution can reduce the basis set and should therefore be used.

4.1. Incorporating special properties of the quantum state

Simplifications arise if the quantum state which produces the Wigner function has certain properties. If $|\psi\rangle$ is an eigenstate of a given Hamiltonian \hat{H} with energy E_n , then the semiclassical considerations in the following section show that the Gaussian centres may be restricted to $|H(X) - E_n| \leq \hbar$.

If $|\psi\rangle$ is itself a linear combination of, e.g., two states, $|\psi\rangle = a_1|\psi_1\rangle + a_2|\psi_2\rangle$, the present approach allows one to fit the two states $|\psi_i\rangle$ separately to a set of Gaussians.

A further simplification results from possible symmetries. For instance, for the eigenstate of an even potential, one should place the Gaussians symmetrically at $(P_j, \pm Q_j)$ with $a_{j-} = \pm a_{j+}$, so as to guarantee even or odd states. Again, this is a very particular case, but time reversal invariance is much more common. If the state $|\psi\rangle$ resulted from initial real wavefunctions and the evolution proceeded through interactions that preserve time reversal symmetries (in usual practice, if there are no magnetic fields) then the final state can also be real. In this case, one must choose symmetric pairs of Gaussians at $(\pm P_j, Q_j)$ with equal real coefficients, $a_{j-} = a_{j+}$, so as to ensure that $|\psi\rangle$ is also real. This halves the number of independent coherent states to be fitted and reduces the choice of phase to either zero, or π . Any further knowledge should generally be used to reduce the randomness of the positions of the coherent states to be fitted to $|\psi\rangle$. The semiclassical considerations in the following section may be a further guideline. When this knowledge is exhausted, the best course is

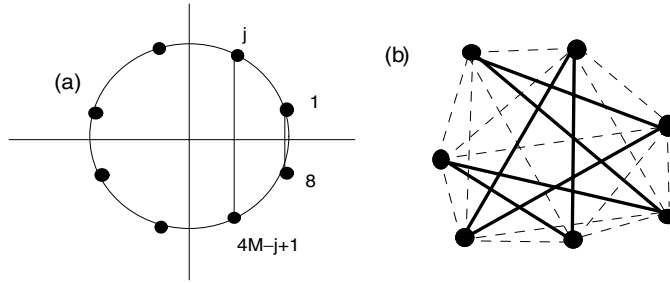


Figure 1. Schematic representation of a regular (a) and random (b) arrangement of Gaussian centres and the resulting chords (dashed) in the plane of phase space. The solid lines indicate the chords used to construct the phases, see text. For the specific example drawn in (a) $M = j = 2$.

to optimize random guesses by Monte Carlo fitting of arbitrary Gaussians, within the given constraints.

4.2. Harmonic oscillator: regularly placed Gaussians on a circle and the problem of degenerate chords

Before we demonstrate the full potential of the proposed method, we first illustrate the points raised above with the simple harmonic oscillator. Here, for a given quantum state $|\psi_n\rangle$, the Husimi distribution

$$H^{\psi_n}(x) = \exp(-x^2/2) \frac{1}{n!} (x^2/2)^n \tag{23}$$

peaks at a circle in phase space with radius $x = R_n$, where $\frac{1}{2}R_n^2 = \frac{1}{2}(p^2 + q^2) \equiv n$ is the classical energy close to the quantum energy of $E_n = n + \frac{1}{2}$. Moreover, the problem is time reversal invariant and has parity in space. A coherent state basis on a circle in phase space with fixed radius R_n and compatible with the two symmetries is given by

$$\{|X_j\rangle\} = \left\{ \left| R_n, \phi_j = \frac{2j-1}{4M}\pi \right. \right\}, \quad 1 \leq j \leq 4M, \tag{24}$$

where $M \geq 1$ is an integer and $P_j = R_n \sin \phi_j$, $Q_j = R_n \cos \phi_j$. The explicit coordinate representation follows directly from (4). In the remaining angular degree of freedom, the spatial inversion operation $q \rightarrow -q$ translates on the basis states to $\phi_j \rightarrow \phi_j + \pi$ while time reversal leads to $\phi_j \rightarrow -\phi_j$. Each coherent state j carries the same absolute weight $A_j(R_n) = A(R_n)$ which follows from the simplest solution to the matrix equation (16). This weight may be absorbed in the normalization constant $N(R_n)$ of the wavefunction to be constructed. The determination of the phases θ_j of the coefficients a_j is greatly simplified by the symmetry of the wavefunction. From figure 1(a) it is clear that the two chords shown connect gpps related by time reversal symmetry, i.e.

$$(a_j |R_n, \phi_j\rangle)^* = a_j^* |R_n, -\phi_j\rangle = a_j^* |R_n, \phi_{4M-j+1}\rangle. \tag{25}$$

This implies $\theta_j = -\theta_{4M-j+1}$. A second condition on the phases is provided by the general chord relation (22). Since the chord function \tilde{W}^ψ is real for the harmonic oscillator⁵, one can fulfil (22) only if the phase on the rhs obeys

$$\theta_j - \theta_k + \frac{1}{2}R^2 \sin \frac{(j-k)\pi}{2M} = m\pi, \tag{26}$$

⁵ This may be inferred from the fact that complex conjugate of the rhs of (17) is identical to the original expression since the Wigner function for the harmonic oscillator is real [15].

Table 1. Comparison of the accuracy σ as defined by (15) of HO eigenfunctions ψ_n approximated with N regularly spaced and randomly chosen (bold) ggps, see text.

n	N	σ	R_n
1	4	9.9×10^{-2}	3.33
	4	1.0×10^{-2}	
	8	2.4×10^{-2}	
4	(8^a)	9.2×10^{-3}	3.90
	8	3.30×10^{-2}	
	8	1.45×10^{-3}	
6	8	9.0×10^{-2}	4.44
	8	9.5×10^{-3}	

^a Optimization produces some negative weights A_j indicating overlapping ggps.

where we put without loss of generality $m = 0$ since we can fix the sign of the terms in the linear combination in the end.

These two conditions for the phases of a chord completely determine θ_j for the ggp in the first quadrant of phase space,

$$\theta_j = -\frac{R^2}{4\hbar} \sin 2\phi_j \quad (j \leq M). \tag{27}$$

The two symmetries yield the phases in the other three quadrants. The resulting wavefunction for the HO is

$$\Psi_n(q) = N(R_n) \sum_{j=1}^M \{\psi_j(r_j(q)) + (-1)^n \psi_j(r_j(-q))\}, \tag{28}$$

with

$$\psi_j(r_j(q)) = \exp(-r_j^2/2\hbar) \cos(r_j R_n \sin \phi_j/\hbar), \quad r_j = q - R_n \cos \phi_j. \tag{29}$$

The constant $N(R_n)$ is fixed by requiring Ψ_n to be normalized. It is easy to see that for ($n = 0, R_0 = 0$) the exact HO ground state wavefunction results. For excited states we find the best radius R_n where the overlap $\langle \Psi_n | \Psi_n^{\text{exact}} \rangle$ has its maximum as a function of R_n .

In this way, we have determined the approximate HO eigenfunctions (28) for $n = 1, 4, 6$ and compared their error σ according to (15) in table 1 with the error for approximate eigenfunctions constructed from randomly placed Gaussians. One sees that in general the accuracy increases with the number N of coherent states on the circle. For a given N the basis with randomly distributed Gaussians, whose construction we will describe next, is always superior by roughly one order of magnitude in σ .

4.3. Harmonic and Morse oscillator: randomly placed Gaussians

Now, on purpose we do not make any use of our knowledge about symmetries etc to assess how the ‘black box’ Monte Carlo method for placing the Gaussians performs in the general situation, illustrated in figure 2. Specifically, we study excited states of a harmonic (HO) and a Morse (MO) oscillator where the latter supports 18 bound states defined in atomic units ($\omega = m = \hbar = 1$).

To determine the centres $x_k = (p_k, q_k)_{k=1, \dots, N}$ of the Gaussians, we perform a Monte Carlo sampling restricted by two conditions: (i) centres are only accepted in a region where the distribution is significant, i.e. where the distribution exceeds a certain threshold δ ; (ii) the centres must not be too close; this means a minimum distance Δ between centres is fixed

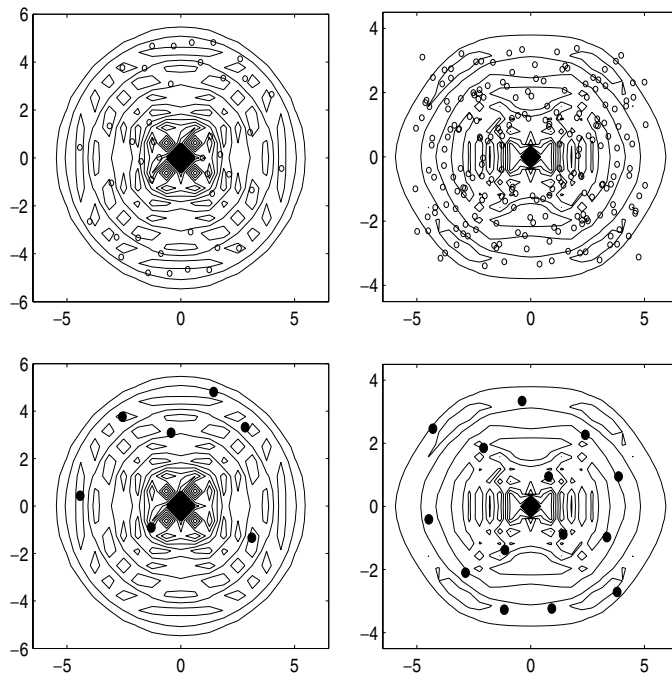


Figure 2. Contour plot of chord functions shown as solid lines (18) for the third excited HO state (left) and the fifth excited MO state (right). In the top row, the open circles give the position of all $N(N - 1)/2$ chords, measured from the origin $(0, 0)$ in the centre ($N = 7$ for HO, $N = 14$ for MO). In the bottom row, the filled circles indicate the N largest chords used for constructing the polygon to determine the phases.

a priori, thereby avoiding overlaps and reducing the total number N of gpps used for the representation.

In the practical implementation we begin with one centre $N = 1$, determine the a_j as described in section 3 and increase N until the desired accuracy σ in (15) is reached.

Figure 3 (top) shows the known Husimi function for the third excited state of HO (left) and for the fifth excited state of MO (right). On the bottom the corresponding fitted distributions are shown. We found that $N = 7$ is sufficient to reproduce quite well the Husimi function of HO whereas 14 coherent states (gpps) are needed in the MO example, to achieve a global relative error of $\sigma \leq 0.01$ according to (15). The respective values for the threshold δ and the minimum distance Δ are given in the caption of figure 3.

Figure 4 shows the Wigner function of the third excited state of the HO together with its corresponding fit obtained with 7 gpps. The present fitting reproduces the Wigner function everywhere in phase space, even for negative regions which are signatures of quantum interference. This is clearly illustrated in figure 5 where the deviations of the Monte Carlo sampled Wigner function, less than 10^{-4} everywhere in phase space, are depicted for both the HO (left, $n = 3$) and the MO (right, $n = 5$). The global relative error σ does not exceed 0.01. As one can see from table 1, the basis with N randomly placed Gaussians is always superior for HO eigenstates compared to a basis with N Gaussians regularly distributed on a circle in phase space.

However, for a fixed width of the Gaussians, as used for simplicity in this work, increasing N leads to an improvement of the result only as long as the Gaussians do not significantly

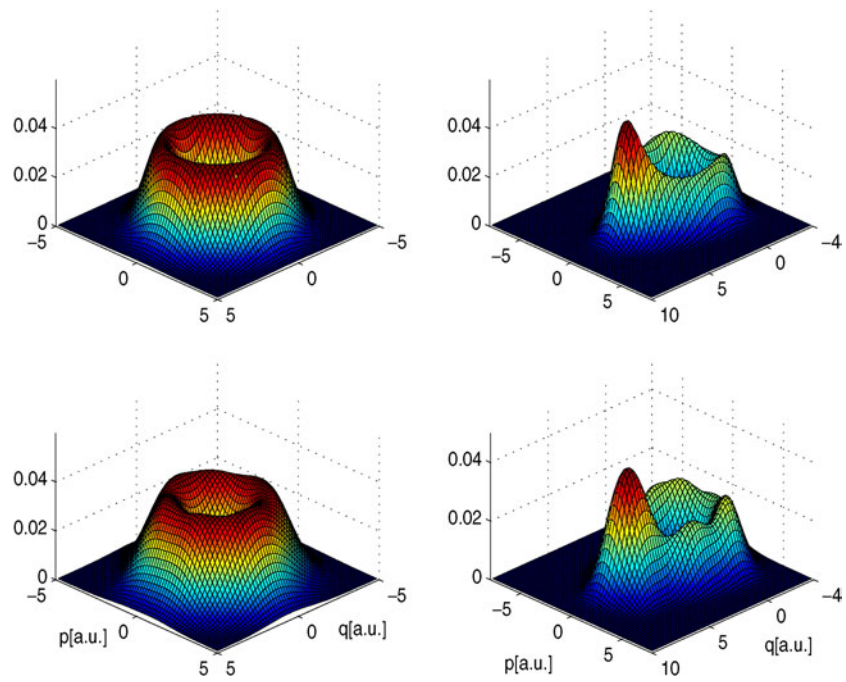


Figure 3. Husimi distributions of the third excited state of the harmonic oscillator (HO) and for the fifth excited state of the Morse oscillator (MO); (top: original, bottom: fit). The fitting of HO (left) is reproduced with $N = 7$ ($\delta = 0.035$, $\Delta = 0.5$) and that of MO (right) with $N = 14$ ($\delta = 0.02$, $\Delta = 1.3$).

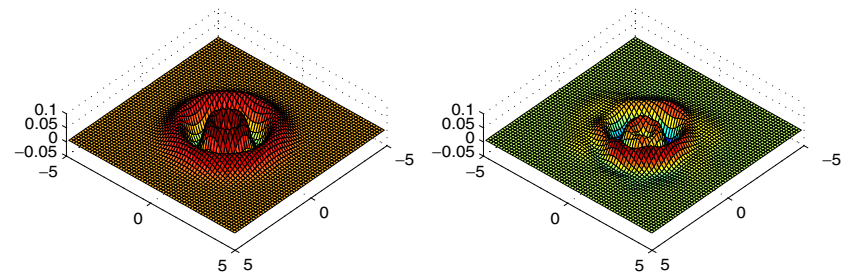


Figure 4. Wigner distributions of the third excited state of HO (left) and its corresponding fit (right) with $N = 7$ as in figure 1.

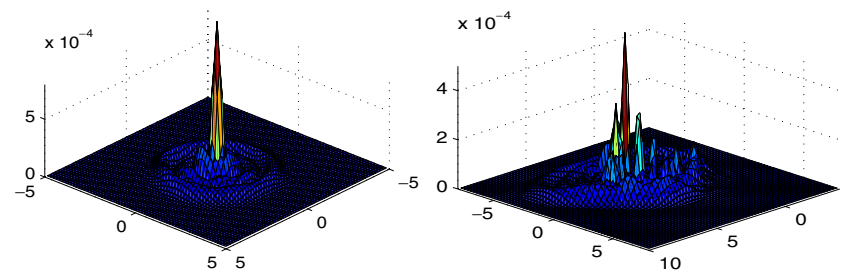


Figure 5. Deviations $s(x)$ according to (15) of the Monte Carlo sampled Wigner function for the third excited HO state (left) and the fifth excited MO state (right) from the exact Wigner function.

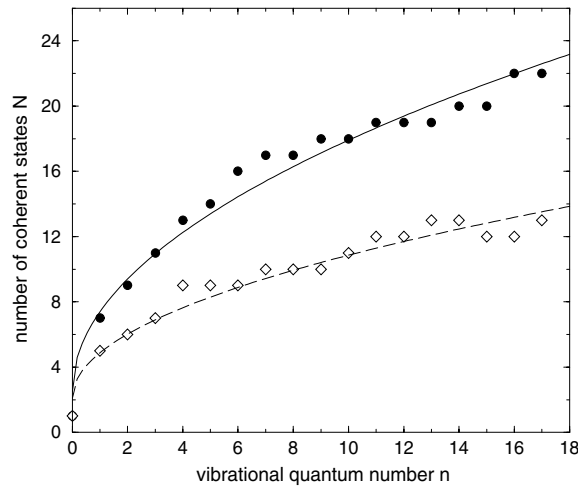


Figure 6. Number of coherent states N used for the fitting versus the vibrational quantum number n for both harmonic oscillator (\diamond , dashed line: fit with $N = 2.77\sqrt{n} + 2.10$) and Morse oscillators (\bullet , solid line: fit with $N = 4.87\sqrt{n} + 2.51$).

overlap. Once this happens, the diagonalization (16) produces unphysical *negative* values for A_j which are illustrated in table 1 with the extreme example of $n = 1$, $N = 8$. Obviously, if one is interested in higher absolute accuracy of the wavefunction and is willing to increase N , one can use Gaussians with smaller widths.

Another problem which may occur can also be easily solved. Although not likely due to the Monte Carlo sampling of the centres for the Gaussians, in some cases it may accidentally happen that $\delta X_{jk} = X_j - X_k$ close to $\delta X_{lm} = X_l - X_m$. In such a case of near degeneracies between δX_{jk} and δX_{lm} we solve the 2×2 linear equations

$$\begin{aligned}\tilde{W}'(\delta X_{jk}) &= B_{jk}\tilde{W}_{jk}(\delta X_{jk}) + B_{lm}\tilde{W}_{lm}(\delta X_{jk}) \\ \tilde{W}'(\delta X_{lm}) &= B_{jk}\tilde{W}_{jk}(\delta X_{lm}) + B_{lm}\tilde{W}_{lm}(\delta X_{lm}),\end{aligned}\quad (30)$$

for the phases θ_{jk} and θ_{lm} in

$$B_{jk} = a_j a_k^* = \sqrt{A_j A_k} \exp(i\theta_{jk}), \quad (31)$$

where

$$\tilde{W}'(\delta X_{jk}) = \tilde{W}^\psi - \sum_l |a_l|^2 \tilde{W}_{ll}(\delta X_{jk}). \quad (32)$$

This treatment can be easily generalized to higher chord degeneracies.

Finally, to elucidate the systematic connection between the excitation n of the eigenstate ψ_n and the number of ggps N necessary to represent it, we have calculated $N(n)$ under the constraint that $\sigma < 0.01$. In figure 6 one sees that $N \propto \sqrt{n}$ as the vibrational quantum number n increases. This can easily be understood semiclassically. In fact, the result is generally valid as one can see from the WKB quantization.

5. Semiclassical approach

A semiclassical state $|\psi\rangle_{SC}$ is supported by a curve in phase space, in the case of one degree of freedom, or in general by a surface with half the phase space dimension [10, 11]. If the

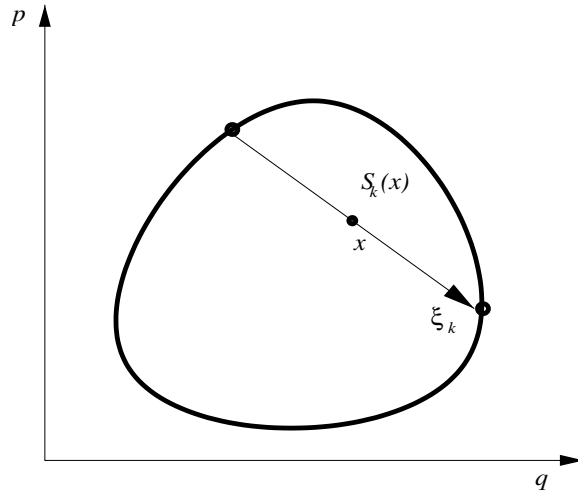


Figure 7. Geometrical illustration of the chord $\xi_k(x)$ in phase space $x(p, q)$.

curve or surface is closed, it must be Bohr-quantized and it will be symmetric about $p = 0$ in the case of time reversal symmetry. In the case of the position representation, for each branch of the curve (surface), $p_j(q)$, one defines the action

$$\mathcal{S}_j(q) = \int_{q_0}^q p_j dq, \tag{33}$$

leading to the generalized WKB wavefunction,

$$\langle q|\psi\rangle_{SC} = \sum_j a_j(q) \exp\left(\frac{i}{\hbar}\mathcal{S}_j(q)\right). \tag{34}$$

The amplitudes $a_j(q)$ can also be expressed in terms of the actions, but the important point is that they are purely classical so that the only \hbar -dependence occurs in the exponential. Thus locally, for any small range of positions, the semiclassical wavefunction reduces to a superposition of plane waves characterized by the wave vectors $p_j(q)/\hbar$. The semiclassical Wigner function is also defined in terms of an action $\mathcal{S}_j(x)$ with respect to the classical curve (surface). But instead of the area between the curve and the q -axis, we are now concerned with the area sandwiched between the curve and one of its chords. The latter, $\xi_k(x)$, is selected by the property that it is centred on the point x , as shown in figure 7. Thus, for one degree of freedom [12],

$$W^\psi(x)_{SC} = \sum_k A_k(x) \cos\left(\frac{\mathcal{S}_k(x)}{\hbar} - \frac{\pi}{4}\right), \tag{35}$$

with straightforward generalizations [13]. The important point is that [7]

$$\frac{\partial \mathcal{S}_k}{\partial x} = \mathbf{J}\xi_k, \tag{36}$$

where we use the symplectic matrix \mathbf{J} defined in (9). Thus the semiclassical state is again represented by a superposition of waves, but now these are *phase space waves*:

$$W^\psi(\delta x)_{SC} \approx \sum_k A_k(x) \cos\left(\frac{\delta x \wedge \xi_k(x)}{\hbar} - \frac{\pi}{4}\right). \tag{37}$$

Here δx is measured from the chord centre, so that comparison of this expression with (22) immediately reveals that these waves have exactly the same wave vector as a pair of Gaussians at the tip of each chord $\xi_k(x)$. It follows that an important feature of a semiclassical state is automatically reproduced by fitting it with Gaussians precisely placed on the corresponding classical curve (surface). Note that, in fact, this is a major *a priori* obstacle to performing the fitting, because the oscillations near the midpoint of a long chord are very fine for $\hbar \ll S_k$. One would need very narrow Gaussians indeed to fit these phase space waves directly, rather than having them arise naturally as interferences. All that is left to determine is the phase: $S_k/\hbar - \pi/4$. How can we single out the region in which to place the gpps, if we have no *a priori* knowledge of the classical structures corresponding to a quantum state? The obvious course is to smooth the Wigner function with a Gaussian window. In other words, we initially fit the Husimi function. Recalling that the gpps have linear width of order $\sqrt{\hbar}$, while the wavelength of the Wigner oscillations is $\hbar/|\xi_k|$, it follows that this Gaussian window erases effectively a semiclassical Wigner function, except in the limit of very small chords. This is a simple explanation of the well-known fact that only in the neighbourhood of the classical curve (surface) itself is the semiclassical Husimi function appreciable. In the simple case of one degree of freedom, the Husimi function is concentrated near the energy shell. Thus, by fitting gpps to a Husimi function, one automatically samples its relevant classical manifold, if it happens to have a (possibly unknown) semiclassical structure. A basic assumption in the above argument is that the gpps along the curve (surface) are neither too crowded, to avoid confusing superpositions, nor too sparsely spaced, lest gaps should arise in the fitting. It is thus easy to estimate the growth of the number of coherent states required to fit the eigenstate $|\psi_n\rangle$ with the degree of excitation. Since the linear width of the Gaussian scales as $\sqrt{\hbar}$, the phase space area of the curve grows as $n\hbar$ and hence its length grows as $\sqrt{n\hbar}$, the number of equispaced Gaussians needed to cover the curve grows as \sqrt{n} . Of course, we have assumed here that the shape of the curve does not change with n , as for the harmonic oscillator. If the eigencurve elongates for higher excitation, the number of gpps necessary for a good fit will grow as n^α , with $1/2 \leq \alpha \leq 1$. We can also estimate the growth in time of the number of gpps required to fit an evolving semiclassical state with arbitrary precision. According to the theory of van Vleck [10], it is sufficient to evolve the curve (surface) classically and then to reconstruct the wavefunction. This principle can also be applied to Wigner functions, according to Berry and Balazs [14]. If the driving Hamiltonian is chaotic, then the curve will stretch at a rate depending on the Lyapunov exponent, λ . Clearly, this also determines the initial rate of growth of the number of gpps needed for an adequate fit. Ultimately, when the curve densely covers all the available phase space (the energy shell of the driving Hamiltonian), a relatively steady state will be reached where the number of gpps saturates.

6. Conclusions

Optimal fitting of quantum states by phase space Gaussians is achieved by first fitting the Husimi function and then determining the quantum phases from the chord function, i.e. the Fourier transform of the Wigner function. The density of Gaussians in phase space must be finely adjusted: if there are too few, essential features of the state will be missed, whereas an excessive number of Gaussians would introduce interference terms in the Husimi function itself, which could only be accommodated by a much more complex variation of this method. The numerical examples in section 4 indicate clearly that, in addition to achieving excellent overall accuracy, all essential qualitative features of the states are captured by this method, using a basis of Gaussians that grows more slowly than the excitation number of the fitted states. This last result and further insight into the fitting procedure follows from

the semiclassical analysis in the previous section. This can be generalized readily to states of quantum systems with higher degrees of freedom if these are eigenstates of integrable systems (i.e. if they are supported by a Lagrangian surface in phase space, see, e.g., [11]). Of course, more Gaussians will then be needed for the fitting, but the preliminary fit of the Husimi function should still provide optimal results. From a fundamental point of view the potential for this method to deal with the eigenstates of chaotic systems is even more interesting. Though the *chord* and *centre* description of the Wigner function still applies to linear combinations of eigenstates over narrow energy windows, no classical theory accounts for individual eigenstates at present. Therefore, it will be extremely useful to describe these as interfering superpositions of Gaussians placed near the energy shell. Of course, the size of this basis would diverge at the classical limit as $\hbar \rightarrow 0$, but manageable approximations should be attainable for finite excitations. Although we have restricted the discussion and examples to pure states it is worthwhile to note that with the described expansion it is also possible to represent mixed states by Gaussians.

Acknowledgments

AK gratefully acknowledges the financial support of the Alexander von Humboldt (AvH) Foundation/Bonn-Germany, under the grant of Research fellowship no IV.4-KAM 1068533 STP. AMOA thanks the MPIPKS-Dresden for a Martin Gutzwiller Fellowship, during which this work was initiated, and acknowledges support from CNPq and Pronex in Brazil.

References

- [1] Horenko I, Schmidt B and Schuette C 2002 *J. Chem. Phys.* **117** 4643
- [2] Szabo S, Adam P, Janszky J and Domokos P 1996 *Phys. Rev A* **53** 2698
- [3] Cohen Tannoudji C, Diu B and Laloe F 1977 *Quantum Mechanics* (New York: Wiley)
- [4] Schleich W P 2001 *Quantum Optics in Phase Space* (Berlin: Wiley VCH)
Lee H-W 1995 *Phys. Rep.* **259** 205
- [5] Moyal J E 1949 *Proc. Camb. Phil. Soc. Math. Phys. Sci.* **45** 99
- [6] Press W H, Teukolsky S A, Vetterling W T and Flannery B P 1992 *Numerical Recipes in Fortran* (Cambridge: Cambridge University Press) p 22
- [7] Ozorio de Almeida A M 1998 *Phys. Rep.* **295** 265
- [8] Marks R J II, Walkup J F and Krile T F 1977 *Appl. Opt.* **16** 746
- [9] Radmore P M and Barnett S M 1997 *Methods in Theoretical Quantum Optics* (Oxford: Oxford University Press)
- [10] Van Vleck J H 1928 *Proc. Math. Acad. Sci. USA* **14** 178
- [11] Ozorio de Almeida A M 1988 *Hamiltonian Systems: Chaos and Quantization* (Cambridge: Cambridge University Press)
- [12] Berry M V 1977 *Phil. Trans. R. Soc.* **287** 237
- [13] Ozorio de Almeida A M and Hannay J H 1982 *Ann. Phys., NY* **138** 115
- [14] Berry M V and Balazs N L 1979 *J. Phys. A: Math. Gen.* **12** 625
- [15] Hug M, Menke C and Schleich W P 1998 *Phys. Rev A* **57** 3188